Biochemical Pharmacology 79 (2010) 908–920

Contents lists available at ScienceDirect

Biochemical Pharmacology

journal homepage: www.elsevier.com/locate/biochempharm

Characterization of endogenous calcium responses in neuronal cell lines

Irina Vetter, Richard J. Lewis *

Institute for Molecular Bioscience, The University of Queensland, St Lucia, Queensland 4072, Australia

ARTICLE INFO

Article history:
Received 18 September 2009
Accepted 21 October 2009

Keywords:
Endogenous
Neuronal cell line
Characterization
Calcium
Receptor
Ion channel

ABSTRACT

An increasing number of putative therapeutic targets have been identified in recent years for the treatment of neuronal pathophysiologies including pain, epilepsy, stroke and schizophrenia. Many of these targets signal through calcium (Ca^{2+}), either by directly facilitating Ca^{2+} influx through an ion channel, or through activation of G proteins that couple to intracellular Ca^{2+} stores or voltage-gated Ca^{2+} channels. Immortalized neuronal cell lines are widely used models to study neuropharmacology. However, systematic pharmacological characterization of the receptors and ion channels expressed in these cell lines is lacking. In this study, we systematically assessed endogenous Ca^{2+} signaling in response to addition of agonists at potential therapeutic targets in a range of cell lines of neuronal origin (ND7/23, SH-SY5Y, 50B11, F11 and Neuro2A cells) as well as HEK293 cells, a cell line commonly used for over-expression of receptors and ion channels. This study revealed a remarkable diversity of endogenous Ca^{2+} responses in these cell lines, with one or more cell lines responding to addition of trypsin, bradykinin, ATP, nicotine, acetylcholine, histamine and neurotensin. Subtype specificity of these responses was inferred from agonist potency and the effect of receptor subtype specific antagonist. Surprisingly, HEK293 and SH-SY5Y cells responded to the largest number of agonists with potential roles in neuronal signaling. These findings have implications for the heterologous expression of neuronal receptors and ion channels in these cell lines, and highlight the potential of neuron-derived cell lines for the study of a range of endogenously expressed receptors and ion channels that signal through Ca^{2+}.

1. Introduction

In recent years, an increasing number of receptors and ion channels expressed on central or peripheral neurons have been identified as putative therapeutic targets for the treatment of neuronal pathophysiologies such as chronic pain, stroke, epilepsy and schizophrenia. These targets include transient receptor potential channels (e.g. TRPV1), voltage-gated calcium channels (e.g. $Ca_v2.2$ and 3.2), ionotropic glutamate (e.g. NMDA and AMPA receptors) and nicotinic acetylcholine receptors (e.g. α7 and α4 nAChR), as well as numerous G-protein coupled receptors (GPCR) [1–7]. GPCR targets of particular interest include the protease-activated receptors, specifically PAR1, PAR2 and PAR4, which are expressed in dorsal root ganglion (DRG) and central neurons and contribute to a variety of painful conditions, including visceral and arthritic pain and have also been speculated to contribute to epilepsy and blood brain barrier integrity [8–13]. Similarly, interest in bradykinin B1 and B2 receptors has been renewed with the observation that intra-articular administration of a bradykinin B2 antagonist appears promising in the treatment of painful osteoarthritis [14], while bradykinin B1 antagonists may be particularly useful in chronic inflammatory pain [15]. Also emerging as potential therapeutic targets are the neurotensin receptors, with both neurotensin 1 and neurotensin 2 receptors contributing to the antinociceptive effects of neurotensin [16] and the neurotensin analogue contulakin G from *Conus geographus* [17]. In addition, targeting neurotensin receptors has also been suggested as a promising novel approach to treat schizophrenia and epilepsy [18,19]. Additional GPCRs with therapeutic potential in neuronal pathophysiologies such as pain, epilepsy, stroke and schizophrenia include muscarinic acetylcholine receptors [20,21], in particular M2 and M4 receptors which mediate analgesia [22,23]; D2 dopamine receptors [24,25], histamine H1–H3 receptors [26,27], several metabotropic glutamate receptors [28,29],

Abbreviations: Ca^{2+}, calcium ion; GPCR, G-protein coupled receptor; ATP, adenosine triphosphate; TRPV1, transient receptor potential vanilloid 1; PAR, protease-activated receptor; GABA, γ-aminobutyric acid; DMEM, Dulbeccos' Modified Eagle Medium; FBS, foetal bovine serum; PBS, phosphate buffered saline; PSS, physiological salt solution; EDTA, ethylenediaminetetraacetic acid; HAT, hypoxanthine, aminopterin and thymidine; db-cAMP, N6,2′-O-dibutyryladenosine 3′:5′ cyclic monophosphate; NGF, nerve growth factor; BAPTA, 1,2-bis(o-aminophenoxy)ethane-N,N,N′,N′-tetraacetic acid; AFU, arbitrary fluorescence unit; SEM, standard error of the mean; NMDA, N-methyl-D-aspartic acid; pFHHSiD, *p*-fluorohexahydro-sila-difenidol hydrochloride; PLC, phopholipase C; Fluo-4-AM, Fluo-4 acetomethoxyester; HEK293, human embryonic kidney cells; RPMI, Roswell Park Memorial Institute; PDL, Poly-D-lysine.

* Corresponding author. Tel.: +61 7 3346 2984; fax: +61 7 3346 2101.
E-mail addresses: i.vetter@uq.edu.au (I. Vetter), r.lewis@imb.uq.edu.au (R.J. Lewis).

0006-2952/$ – see front matter.
doi:10.1016/j.bcp.2009.10.020

$GABA_B$ receptors [30] and several serotonin 5-HT [31–34] as well as purinergic receptor subtypes [35–39].

Importantly, many of these putative therapeutic targets signal through an increase in intracellular calcium (Ca^{2+}), either by directly facilitating Ca^{2+} influx through an ion channel, or through activation of G proteins that couple to intracellular Ca^{2+} stores or voltage-gated Ca^{2+} channels. This makes assessment of Ca^{2+} fluxes in response to agonists and antagonists at these targets a broadly applicable approach that can be optimized for detailed functional studies as well as the high throughput identification of novel modulators of these targets.

Primary cultures of adult and embryonic neurons are widely used to investigate neuronal pharmacology and signaling mechanisms. However, the culture of primary neurons is not only time-intensive but can also yield cell populations that have undergone variable extents of differentiation associated with their removal and culture. In addition, in the case of primary DRG neurons, primary culture yields heterogenous cell populations, which can make identification of neuronal cells that express receptors or ion channels of interest difficult. To gain more reproducible responses, several immortalized dorsal root ganglion and neuroblastoma-derived cell lines have been established that allow the study of the physiology and pharmacology of endogenously expressed receptors and ion channels *in vitro*. While some neuronal cell lines have been used extensively to assess neuronal physiology such as neurotransmitter release, the systematic characterization of Ca^{2+} responses to agonists of endogenously expressed receptors and ion channels is lacking.

In the present study, we have systematically characterized endogenous Ca^{2+} responses to several agonists at GPCRs and ion channels in three dorsal root ganglion-derived neuronal cell lines, F11 [40], ND7/23 [41] and 50B11 [42] cells, as well as the commonly used human neuroblastoma cell lines SH-SY5Y [43] and Neuro2A [44], and HEK293 (human embryonic kidney) cells [45] which are commonly used to express neuronal receptors and ion channels. Surprisingly, Ca^{2+} responses of these cell lines were diverse, with HEK293 and SH-SY5Y cells responding to the largest number of agonists with potential roles in neuronal signaling. Our results highlight the potential of DRG- and neuroblastoma-derived cell lines for the study of endogenously expressed neuronal receptors and ion channels through Ca^{2+} signaling and provide the first systematic evaluation of endogenous Ca^{2+} signaling in commonly used cell lines of neuronal origin.

2. Materials and methods

2.1. Compounds

The following compounds and materials were obtained from the sources indicated: L-glutamine, horse serum, Dulbecco's Modified Eagle Medium (DMEM), Ham's F12, Neurobasal, RPMI (Roswell Park Memorial Institute), 0.25% trypsin/EDTA, B27, foetal bovine serum (FBS), Fluo-4-AM (Fluo-4 acetomethoxyester), phosphate buffered saline (PBS), Invitrogen (Mulgrave, Victoria, Australia); HAT media supplement Hybri-Max™, trypsin, bradykinin, adenosine triphosphate (ATP), nicotine, acetylcholine, choline bitartrate, noradrenaline, dopamine, histamine, glutamate, N-methyl-D-aspartic acid (NMDA), γ-aminobutyric acid (GABA), serotonin, adenosine, substance P, neurotensin, neurokinin A, neurokinin B, capsaicin, Triton-X 100, $MnCl_2$, HOE-140, *p*-fluorohexahydro-sila-difenidol hydrochloride, pyrilamine, pirenzepine (pFHHSiD), BAPTA (1,2-bis(o-aminophenoxy)ethane-N,N,N′,N′-tetraacetic acid), ranitidine, Sigma–Aldrich (Castle Hill, New South Wales, Australia); morphine, David Bull Laboratories Australia (Rowville, Victoria, Australia); nerve growth factor (NGF), GroPep Australia (Thebarton, South Australia, Australia). Capsaicin was prepared as a stock solution in ethanol, with the maximum final ethanol concentration not exceeding 0.001%. All other reagents were prepared as stock solutions in PBS. SLIGRL-NH_2 and TFLLR-NH_2 were a kind gift from Prof. David Fairlie, The Institute for Molecular Bioscience, University of Queensland.

2.2. Cell lines and culture

All cell lines were routinely maintained in antibiotic-free media, with regular testing confirming mycoplasma-free status of cell lines.

HEK293 cells (American Tissue Culture Collection, Manassas, VA, USA) were maintained at 37 °C in a 5% humidified CO_2 incubator in DMEM containing 10% heat-inactivated FBS, 2 mM L-glutamine, pyridoxine and 110 mg/ml sodium pyruvate. Cells were split every 4–6 days or when approximately 90% confluent in a ratio of 1:5 to 1:10 using 0.25% trypsin/EDTA and subcultured into T-75 cm^2 or T-175 cm^2 tissue culture flasks.

SH-SY5Y human neuroblastoma cells, a kind gift from Victor Diaz (Max Planck Institute for Experimental Medicine, Goettingen, Germany), were maintained at 37 °C/5% CO_2 in RPMI containing 15% FBS and 2 mM L-glutamine. Cells were routinely passaged at a 1:5 dilution every 3–5 days using 0.25% trypsin/EDTA (Gibco).

F11 neuroblastoma × DRG neuron hybrid cells were kindly provided by Daniel Kapitzke (School of Pharmacy, The University of Queensland, Australia) and maintained in Ham's F12 media supplemented with 10% FBS, 100 μM hypoxanthine, 0.4 μM aminopterin and 16 μM thymidine (HAT media supplement Hybri-Max™, Sigma–Aldrich, Castle Hill, Australia). F11 cells were passaged at a 1:5 dilution following mechanical dissociation every 2–3 days or when approximately 80% confluent.

ND7/23 neuroblastoma × DRG neuron hybrid cells were obtained from Sigma–Aldrich (Castle Hill, New South Wales, Australia) and grown to approximately 90–95% confluency in DMEM containing 10% heat-inactivated FBS, 2 mM L-glutamine, pyridoxine and 110 mg/ml sodium pyruvate. Confluent cultures were dissociated using 0.25% trypsin/EDTA and split at 1:5 dilution every 3–5 days.

The immortalized DRG sensory neuron cell line 50B11 was a kind gift from A/Prof Ahmet Höke (Departments of Neurology and Neuroscience, Johns Hopkins University, Baltimore, USA). 50B11 cells were maintained in Neurobasal medium (Gibco) supplemented with 10% FBS, 1× B27 (Gibco), 0.5 mM L-glutamine and 0.2% glucose [42]. Cells were grown to approximately 90–95% confluency and dissociated using 0.25% trypsin/EDTA for passaging at 1:3 dilution every 3–5 days. Under these conditions, 50B11 cells remained sensitive to differentiation by forskolin for up to 20 passages.

Neuro2A cells (American Tissue Culture Collection, Manassas, VA, USA) were maintained in DMEM containing 10% heat-inactivated FBS, 2 mM L-glutamine, pyridoxine and 110 mg/ml sodium pyruvate. Cells were split every 4–6 days or when approximately 90% confluent at a 1:2 to 1:4 dilution using 0.25% trypsin/EDTA and subcultured into T-75 cm^2 or T-175 cm^2 tissue culture flasks.

Experiments on each cell line were conducted over a period of several months and spanned on average a minimum of 10–20 passages per cell line. Responses were not significantly affected by passage number, with the exception of histamine responses in SH-SY5Y cells, which were consistent in size during the first 5 passages before becoming variable in subsequent passages.

2.3. Measurement of intracellular Ca^{2+} responses

To assess increases in intracellular Ca^{2+} in response to addition of agonists, cells were seeded on either uncoated (SH-SY5Y and

50B11 cells) or Poly-D-lysine (PDL)-coated (HEK293, ND7/23, F11 and Neuro2A cells) black-walled imaging plates (Corning, Lowell, MA, USA) 48 h prior to the experiment. Seeding densities were 50 000 cells/well (HEK293, ND7/23, F11 and Neuro2A cells), 100 000 cells/well (50B11 cells) or 120 000 cells/well (SH-SY5Y cells), resulting in 90–95% confluent monolayers on the day of Ca^{2+} imaging.

To induce differentiation, media was changed 24 h after plating to DMEM supplemented with 0.5% FBS, 1 mM db-cAMP (N6,2′-O-dibutyryladenosine 3′:5′ cyclic monophosphate) and 2 nM NGF (ND7/23, F11 and Neuro2A cells) or complete Neurobasal media containing 75 μM forskolin (50B11 cells). Microscopic examination of cells differentiated in this manner confirmed extensive neurite outgrowth and neuronal morphology compared to undifferentiated cultures.

Cells were loaded for 30 min at 37 °C with 5 μM Fluo-4-AM in physiological salt solution (PSS; composition NaCl 140 mM, glucose 11.5 mM, KCl 5.9 mM, $MgCl_2$ 1.4 mM, NaH_2PO_4 1.2 mM, $NaHCO_3$ 5 mM, $CaCl_2$ 1.8 mM, HEPES 10 mM) containing in addition 0.3% BSA. To allow for completion of de-esterification, cells were incubated for 10–15 min with PSS. These conditions resulted in good loading for all cell lines assessed, evidenced by good signal-to-noise ratios. After 2 washes with PSS, or Ca^{2+}-free PSS containing 0.5 mM BAPTA to assess ATP responses in the absence of extracellular Ca^{2+}, cells were transferred to the FLIPR^{TETRA} (Molecular Devices, Sunnyvale, CA) fluorescent plate reader and Ca^{2+} responses measured using a cooled CCD camera with excitation at 470–495 nM and emission at 515–575 nM. Camera gain and intensity were adjusted for each plate to yield a minimum of 1000 arbitrary fluorescence units (AFU) baseline fluorescence. Prior to addition of agonists, 10 baseline fluorescence readings were taken, followed by fluorescent readings every second for 300 s.

To normalize fluorescence signals between cell lines, maximum (F_{Max}) and minimum (F_{Min}) fluorescence values were determined for each well. Specifically, to determine maximal fluorescence (F_{Max} values) for each well, 0.3% Triton X-100 was added at the end of each experiment and resultant fluorescence increases monitored for a further 60 s. To determine F_{Min} values, 100 mM $MnCl_2$ was subsequently added and fluorescence monitored for an additional 60 s. Responses were then normalized as described in Section 2.4. F_{Max} values obtained after addition of 0.3% Triton-X were 6099 ± 239 for 50B11 cells, 4242 ± 220 for F11 cells, 2424 ± 118 for Neuro2A cells, 4438 ± 544 for ND7/23 cells, 6559 ± 343 for SH-SY5Y cells and 5729 ± 117 for HEK293 cells (n = 4–6 plates).

To assess putative endogenous Ca^{2+} responses to agonists, an initial screen was carried out using a single agonist concentration approximating literature reported EC_{80} values. Agonists that failed to change the Fluo-4 fluorescence were confirmed a minimum of three times, and full concentration–response curves were determined for responders. For each concentration–response curve, Ca^{2+} responses were assessed in at least triplicate and confirmed in at least 3 independent experiments.

2.4. Data analysis

Unless otherwise stated, all data are expressed as mean ± standard error of the mean (SEM) either from a single representative experiment or averaged data from at least three separate experiments. Unless otherwise stated, statistical significance was determined using an unpaired, two-tailed Student's t-test, with statistical significance defined as $p < 0.05$.

To enable comparison of the magnitude of responses between cell lines, raw fluorescence values were converted to % F_{Max} values using $(F - F_{Min})/(F_{Max} - F_{Min}) \times 100$ where F is the fluorescence

Table 1
Characterization of endogenous Ca^{2+} responses in cell lines of neuronal origin[a].

	ND7/23		F11		50B11		SH-SY5Y		Neuro2A		HEK	
	pEC_{50}	% F_{Max}	pEC_{50}	% F_{Max}	pEC_{50}	% F_{Max}	pEC_{50}	% F_{Max}	pEC_{50}	% F_{Max}	pEC_{50}	% F_{Max}
Acetylcholine	–		–		–		6.7 ± 0.2	29.6–46.4	–		7.1 ± 0.02	57.9–65.0
ATP	–		4.9 ± 0.1	26.0–41.7	4.9 ± 0.1	1.5–6.8	–		5.2 ± 0.5	1.8–3.5	6.0 ± 0.1	40.6–55.0
Bradykinin	8.3 ± 0.1	12.6–16.2	11.4 ± 0.1 8.7 ± 0.1	47.2–69.3	–		7.4 ± 0.3	4.1–5.1	6.6 ± 0.07	5.6–6.0	6.9 ± 0.5	6.3–11.4
Choline	–		–		–		5.1 ± 0.2	45.6–71.0	–		–	
Histamine	–		–		–		5.8 ± 0.09	12.3-23.7	–		4.9 ± 0.1	2.7–3.2
Neurotensin	–		–		–		–		–		7.2 ± 0.1	3.2–3.6
Nicotine	–		–		–		5.5 ± 0.04	13.4–29.0	–		–	
Trypsin	–		7.4 ± 0.2	22.6–38.2	–		7.0 ± 0.1	27.6–47.8	7.8 ± 0.02	3.1–3.3	8.3 ± 0.03	67.5–77.1

[a] Ca^{2+} responses to addition of agonists were assessed by monitoring Fluo-4 fluorescence in HEK293, ND7/23, SH-SY5Y, 50B11, F11 and Neuro2A cells using a FLIPR^{TETRA} fluorescence plate reader. Responders and non-responders (–) were determined by initial assessment of approximately literature EC_{80} agonist concentrations. No responses were observed in these cell lines to addition of adenosine, capsaicin, dopamine, GABA, glutamate, morphine, neurokinin A and B, NMSA, noradrenaline, serotonin and substance P. EC_{50}s, maximum response (% F_{Max}) and Hillslope were determined for acetylcholine, ATP, bradykinin, choline, histamine, neurotensin, nicotine and trypsin in responding cell lines. Hillslopes were 1.0 for all agonists except acetylcholine in HEK293 cells (2.2 ± 0.1), ATP in F11 (2.1 ± 0.3) and HEK293 cells (2.2 ± 0.9), choline in SH-SY5Y (2.7 ± 0.3) and trypsin in F11 cells (3.3 ± 0.8). Data are presented as range (% F_{Max}) or mean ± SEM (pEC_{50}) of 3 independent experiments.

after agonist addition and F_{min} is the fluorescence after addition of $MnCl_2$, which was generally comparable to baseline fluorescence. To establish concentration–response curves, the maximum increase in % F_{Max} after addition of agonist was plotted using GraphPad Prism Version 4.01 and a 4-parameter Hill equation either with Hill coefficient = 1, a variable slope, or a two-site fit was fitted to the data. For statistical comparison of best-fit values for the different concentration–response curves, the comparison function of GraphPad Prism was used to compute the *F*-test value, with statistical significance defined as $p < 0.05$.

3. Results

Endogenous Ca^{2+} responses to 19 agonists of ligand-gated ion channels and G-protein coupled receptors were assessed in HEK293, SH-SY5Y, ND7/23, 50B11, F11 and Neuro2A (Table 1). Initially, responses to approximately literature EC_{80} concentrations of agonists were assessed to identify responders and non-responders, followed by generation of full concentration–response curves for agonists eliciting detectable Ca^{2+} responses. Specifically, Ca^{2+} responses to addition of trypsin (1 μM), bradykinin (100 μM), nicotine (100 μM), acetylcholine (10 μM), noradrenaline (100 μM), dopamine (1 mM), histamine (1 mM), glutamate (1 mM), NMDA (1 mM), GABA (1 mM), serotonin (1 mM), adenosine (100 μM), ATP (1 mM), substance P (100 μM), neurotensin (1 μM), neurokinin A and B (1 μM), capsaicin (300 nM) and morphine (1 μM) were assessed by monitoring Fluo-4 fluorescence using the $FLIPR^{TETRA}$ fluorescence plate reader. One or more cell lines responded with either transient or sustained Ca^{2+} increases to addition of trypsin, bradykinin, ATP, nicotine, acetylcholine, histamine and neurotensin (Figs. 1–8). No increases in intracellular Ca^{2+} were observed in response to addition of

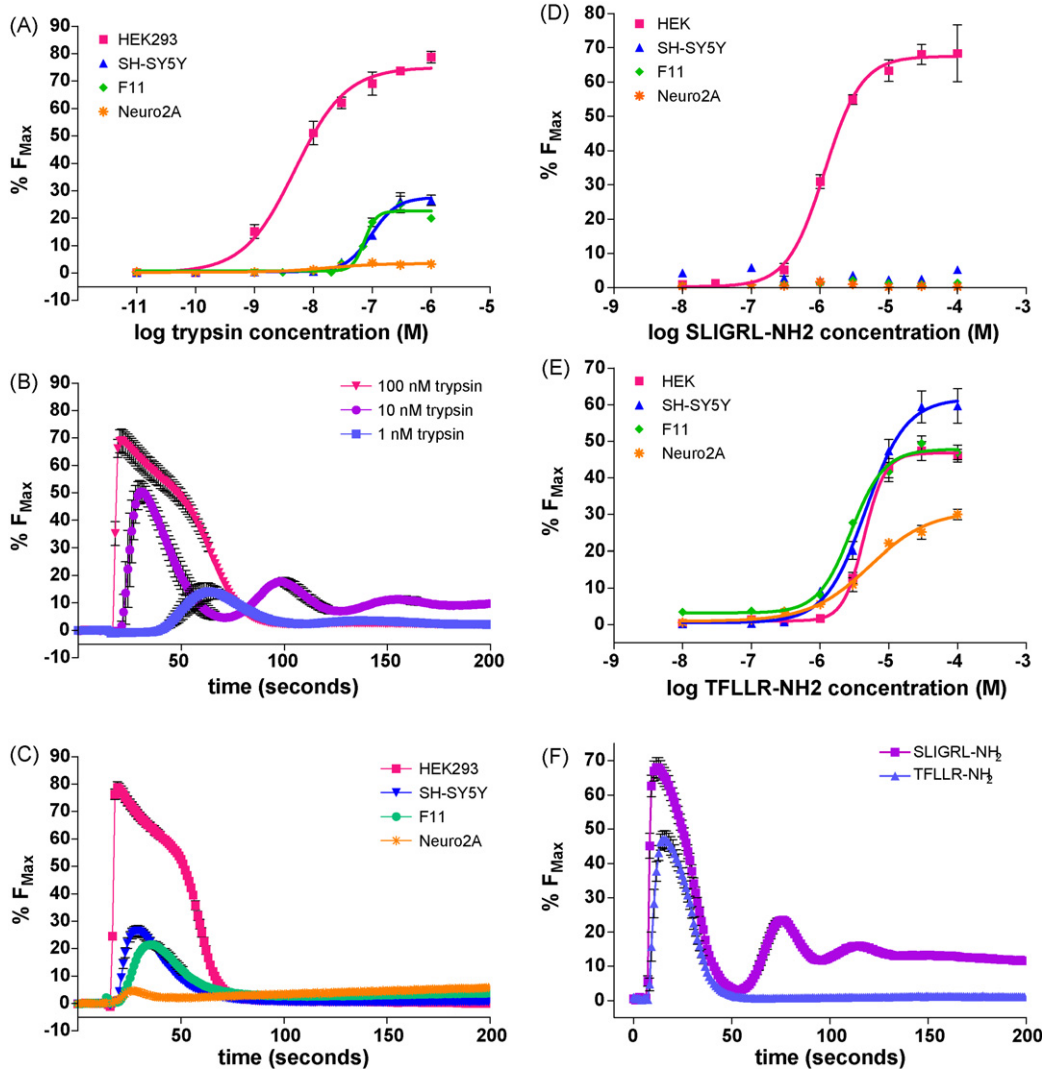

Fig. 1. Trypsin elicits Ca^{2+} transients in HEK293, SH-SY5Y, F11 and Neuro2A cells. (A) Addition of trypsin caused concentration-dependent increases in intracellular Ca^{2+} in HEK293, SH-SY5Y, F11 and Neuro2A but not ND7/23 and 50B11 cells. Trypsin-mediated Ca^{2+} responses were largest in HEK293 cells, intermediate in SH-SY5Y and F11 cells and of relatively small magnitude in Neuro2A cells. (B) Addition of trypsin to HEK293 cells caused concentration-dependent Ca^{2+} oscillations, with high (100 nM) concentration leading to rapid and sustained elevations in Ca^{2+} (red trace), while repeated peaks were observed upon addition of 10 nM trypsin (purple trace). Low (1 nM) trypsin concentrations caused small transient with delayed onset (blue trace). (C) Representative Ca^{2+} transients to addition of 1 μM trypsin in HEK293 (red trace), SH-SY5Y (blue trace), F11 (green trace) and Neuro2A (orange trace) cells. (D) Addition of the PAR2-selective agonist SLIGRL-NH_2 caused a measurable increase in intracellular Ca2+ in HEK293, but not SH-SY5Y, F11 or Neuro2A cells. (E) The PAR1-specific agonist elicited responses in HEK293, SH-SY5Y, F11 and Neuro2A cells. (F) HEK293 cells responded to addition of SLIGRL-NH_2 (purple; 1 μM) and TFLLR-NH_2 (blue; 1 μM) with concentration-dependent transient increases in intracellular Ca^{2+}. While TFLLR-NH_2 lead to only a single Ca^{2+} transient, SLIGRL-NH_2, similar to trypsin, caused concentration-dependent Ca^{2+} oscillations in HEK293 cells. Data are presented as mean ± SEM of n = 3–4 wells and are representative of 3 independent experiments. (For interpretation of the references to color in this figure legend, the reader is referred to the web version of the article.)

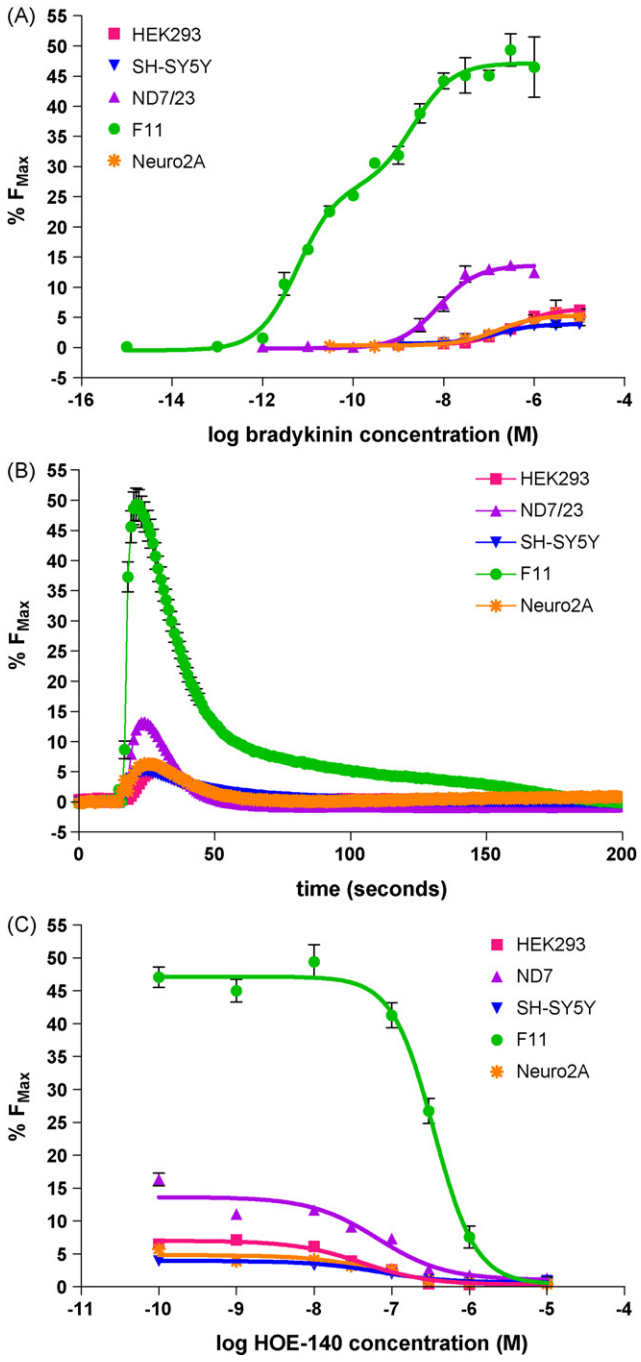

Fig. 2. Bradykinin elicits Ca^{2+} transients in HEK293, SH-SY5Y, ND7/23, F11 and Neuro2A cells. (A) Addition of bradykinin caused concentration-dependent increases in intracellular Ca^{2+} in HEK293, SH-SY5Y, ND7/23, F11 and Neuro2A cells but not 50B11 cells. F11 cells (green) responded to addition of bradykinin with large Ca^{2+} transients that fit preferentially to a two-site fit ($p < 0.05$). Responses in ND7/23 cells (purple) were intermediate, with relatively small responses in Neuro2A (orange), HEK293 (red) and SH-SY5Y (blue) cells. (B) Representative Ca^{2+} transients to addition of 1 μM bradykinin in F11 (green), ND7/23 (purple), Neuro2A (orange), HEK293 (red) and SH-SY5Y (blue) cells. (C) The bradykinin B2 antagonist HOE-140 inhibited bradykinin (1 μM) induced Ca^{2+} transients in a concentration-dependent manner in F11 (green), ND7/23 (purple), SH-SY5Y (blue), HEK293 (red) and Neuro2A (orange) cells. Data are presented as mean ± SEM of $n = 3$–4 wells and are representative of 3 independent experiments. (For interpretation of the references to color in this figure legend, the reader is referred to the web version of the article.)

noradrenaline, dopamine, glutamate, NMDA, GABA, serotonin, adenosine, substance P, neurokinin A and B, capsaicin and morphine in any of the cell lines investigated.

3.1. Trypsin

HEK293, SH-SY5Y, F11 and Neuro2A cells responded to the PAR agonist trypsin with increases in intracellular Ca^{2+}, while 50B11 and ND7/23 cells did not respond (Fig. 1A). The observed EC_{50}s for trypsin-induced Ca^{2+} responses in SH-SY5Y, F11 and Neuro2A cells were 8.9×10^{-8}, 4.1×10^{-8} and 1.7×10^{-8} M, respectively, while trypsin was ~10-fold more potent (EC_{50} of 5.1×10^{-9} M) in HEK293 cells. Trypsin responses in SH-SY5Y, F11 and particularly Neuro2A cells were significantly smaller compared to responses in HEK293 cells (Fig. 1A). In HEK293 cells, addition of intermediate concentrations of trypsin evoked Ca^{2+} oscillations, consistent with IP3-mediated release of Ca^{2+} from intracellular stores through PAR2 (Fig. 1B). In contrast, addition of trypsin to SH-SY5Y, F11 and Neuro2A cells caused a single transient Ca^{2+} increase, consistent with activation of GPCR without Ca^{2+} oscillations (Fig. 1C). In SH-SY5Y, F11 and Neuro2A cells, trypsin did not cause Ca^{2+} oscillations at concentrations from 1 nM to 1 μM. To confirm the PAR subtype(s) involved in mediating responses to trypsin, increases in intracellular Ca^{2+} to the PAR2-specific peptide SLIGRL-NH_2 and the PAR1-specific peptide TFLLR-NH_2 were assessed. Only HEK293 cells responded to addition of SLIGRL-NH_2 with an EC_{50} of 1.1×10^{-6} M, while F11, Neuro2A and SH-SY5Y cells did not respond to SLIGRL-NH_2 (Fig. 1D). In contrast, all cell lines responded to addition of the PAR1 agonist TFLLR-NH_2 with transient increases in intracellular Ca^{2+} (Fig. 1E). The observed EC_{50}s for TFLLR-NH_2-induced Ca^{2+} responses in HEK293, SH-SY5Y, F11 and Neuro2A cells were 5.4×10^{-6}, 5.0×10^{-6}, 3.2×10^{-6} and 5.2×10^{-6} M, respectively. Similar to trypsin responses, SLIGRL-NH_2 caused Ca^{2+} oscillations in HEK293 cells, while TFLLR-NH_2 caused a single transient Ca^{2+} increase (Fig. 1F).

3.2. Bradykinin

All cell lines except 50B11 immortalized DRG neurons responded to bradykinin with a transient increase in intracellular Ca^{2+} (Fig. 2A and B). HEK293, SH-SY5Y and Neuro2A cells exhibited small increases in intracellular Ca^{2+} in response to bradykinin and had comparatively high EC_{50} values of 1.4×10^{-7}, 3.8×10^{-8} and 2.3×10^{-7} M, respectively. ND7/23 cells responded with higher magnitude increases in intracellular Ca^{2+}, with a low nanomolar EC_{50} of 7.5×10^{-9} M. F11 cells displayed very large Ca^{2+} transients in response to addition of bradykinin, with responses occurring over a wide range of concentrations. The preferred fit ($p < 0.05$) was a two-site model with EC_{50}s of 1.8×10^{-9} and 3.7×10^{-12} M and an approximate response fraction of 0.5, suggesting the presence of distinct subtypes or two conformational or signaling states of the bradykinin B2 receptors.

The specific bradykinin B2 receptor antagonist HOE-140 inhibited bradykinin (1 μM) responses with an IC_{50} of 4.1×10^{-8} M in HEK293, 7.0×10^{-8} M in SH-SY5Y cells, 5.8×10^{-8} M in ND7/23 and 5.8×10^{-8} M in Neuro2A cells. Surprisingly, bradykinin-induced responses in F11 cells were less sensitive than the other cell lines to inhibition by HOE-140, with an IC_{50} of 3.0×10^{-7} M and, despite a two-site fit for bradykinin, were fully inhibited by HOE-140 (Fig. 2C).

3.3. Acetylcholine

Addition of acetylcholine induced Ca^{2+} responses in SH-SY5Y and HEK293 cells with EC_{50}s of 1.8×10^{-7} and 7.8×10^{-8} M,

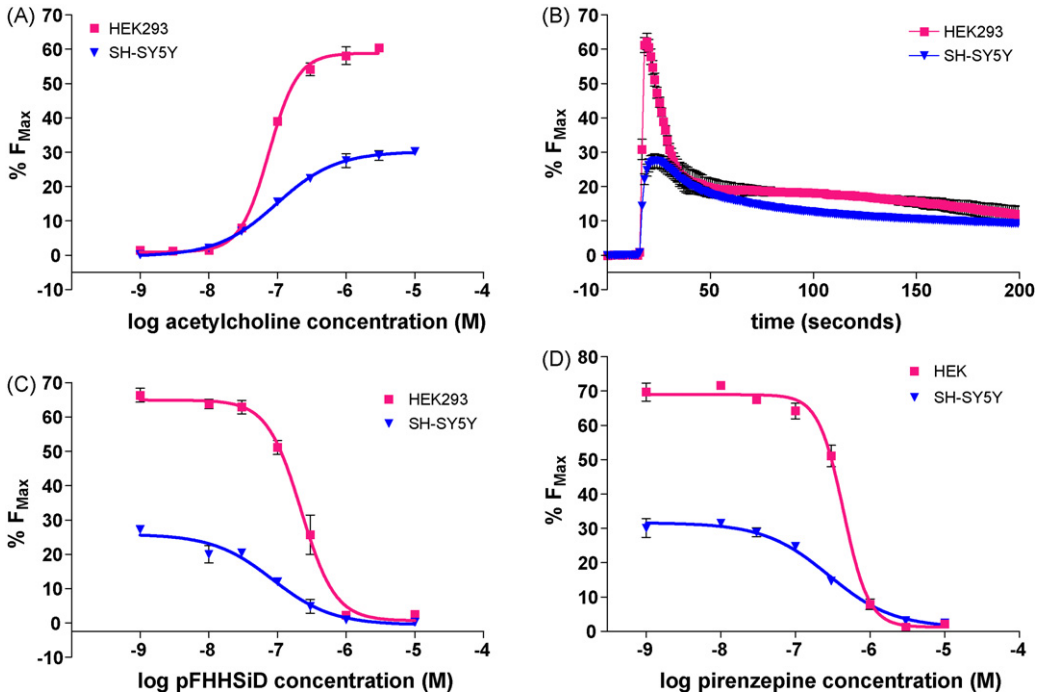

Fig. 3. Acetylcholine elicits Ca^{2+} transients in HEK293 and SH-SY5Y cells by activation of endogenous M3 muscarinic receptors. (A) Addition of acetylcholine evoked concentration-dependent Ca^{2+} transients in HEK293 (red) and SH-SY5Y (blue) cells with approximately equipotent EC_{50}, albeit the magnitude of response was greater in HEK293 compared to SH-SY5Y cells. (B) Representative Ca^{2+} responses caused by addition of 1 μM acetylcholine in HEK293 (red) and SH-SY5Y (blue) cells. (C) The M3 muscarinic antagonist pFHHSiD concentration-dependently inhibited acetylcholine (1 μM)-elicited responses in HEK293 (red) and SH-SY5Y (blue) cells. (D) Consistent with predominant involvement of M3 muscarinic receptors, pirenzepine inhibited acetylcholine-evoked responses in HEK293 and SH-SY5Y cells with IC_{50}s of 1.8×10^{-7} and 2.6×10^{-7} M, respectively. Data are presented as mean ± SEM of n = 3–4 replicates and are representative of 3 independent experiments. (For interpretation of the references to color in this figure legend, the reader is referred to the web version of the article.)

respectively (Fig. 3A and B). While the EC_{50}s for acetylcholine-induced Ca^{2+} responses were similar in both cell lines, the magnitude of the response was significantly ($p < 0.05$) larger in HEK293 (maximum response 60.5 ± 2.2% F_{Max}) compared to SH-SY5Y cells (maximum response 35.9 ± 1.5% F_{Max}). Surprisingly, the M3 receptor-specific antagonist *p*-fluorohexahydro-sila-difenidol hydrochloride (pFHHSiD) completely inhibited acetylcholine-induced responses in both HEK293 and SH-SY5Y cells with similar IC_{50}s of 2.2×10^{-7} and 8.2×10^{-8} M, respectively (Fig. 3C), suggesting a predominant role for M3 muscarinic receptors in acetylcholine-induced responses in these cells. While pFHHSiD is generally considered a M3 muscarinic receptor-specific antagonist, it distinguishes only poorly between M3 and M1 subtypes. Thus, inhibition of acetylcholine-induced responses by the M1-specific antagonist pirenzepine was also assessed. Pirenzepine is typically more potent at M1 (pIC_{50} 7.8–8.5) than M3 (pIC_{50} 6.7–7.1) muscarinic receptors [46–49].

Consistent with predominant involvement of endogenous M3 receptors in HEK293 and SH-SY5Y cells, pirenzepine inhibited the acetylcholine-evoked Ca^{2+} responses with IC_{50}s of 1.8×10^{-7} and 2.6×10^{-7} M (pIC_{50} 6.3 and 6.5), respectively [48,50].

3.4. Nicotine

Of the cell lines tested, only SH-SY5Y neuroblastoma cells responded to the addition of nicotine with an increase in intracellular Ca^{2+} (Fig. 4A and B). Specifically, addition of nicotine induced a transient Ca^{2+} increase with an EC_{50} of 3.1×10^{-6} M. This response was fully inhibited by tubocurarine, partially inhibited by the α3β4 nicotinic antagonists AuIB (10 μM) while methyllycaconitine (100 nM) did not significantly inhibit nicotine-induced Ca^{2+} responses (Fig. 4C). Addition of the α7 nicotinic AChR agonist choline up to 30 μM did not induce a Ca^{2+} response in SH-SY5Y cells (Fig. 5A). However, in the presence of the allosteric α7 modulator PNU120596 (10 μM), choline elicited large Ca^{2+} transients (Fig. 5A and B). We confirmed these Ca^{2+} responses were elicited by α7 receptors, as the α7-selective antagonist methyllycaconitine completely abolished choline-induced responses with an IC_{50} of 2.8×10^{-9} M (Fig. 5C).

3.5. Histamine

Only HEK293 and SH-SY5Y cells responded with increases in intracellular Ca^{2+} following addition of histamine (Fig. 6A and B). EC_{50}s for histamine-induced Ca^{2+} transients differed significantly ($p < 0.05$) between cell lines, with responses in SH-SY5Y cells displaying a higher affinity (EC_{50} 1.4×10^{-6} M) compared to HEK293 cells (EC_{50} 1.4×10^{-5} M). A second component, matching the affinity seen for HEK293 cells, was apparent in some batches of SH-SY5Y cells but did not consistently reach statistical significance over a single-site fit in Prism. The EC_{50} for histamine-induced Ca^{2+} transients in HEK293 cells was 1.4×10^{-5} M and preferably fit a single-site model. Histamine-induced Ca^{2+} transients were generally small, with responses in SH-SY5Y cells significantly larger (maximum response 15.8 ± 2.6% F_{Max}) compared to HEK293 cells (maximum response 3.0 ± 0.2% F_{Max}, $p < 0.05$). The H1-specific antagonist pyrilamine completely inhibited histamine-induced increases in Ca^{2+} in HEK293 with an IC_{50} of 7.0×10^{-9} M (Fig. 6C). In SH-SY5Y cells, pyrilamine inhibited histamine-induced responses with an IC_{50} of 1.6×10^{-9} M (Fig. 6C). In contrast, the H2-specific antagonist ranitidine up to a concentration 10 μM did not affect histamine-induced responses in either SH-SY5Y or HEK293 cells (Fig. 6D).

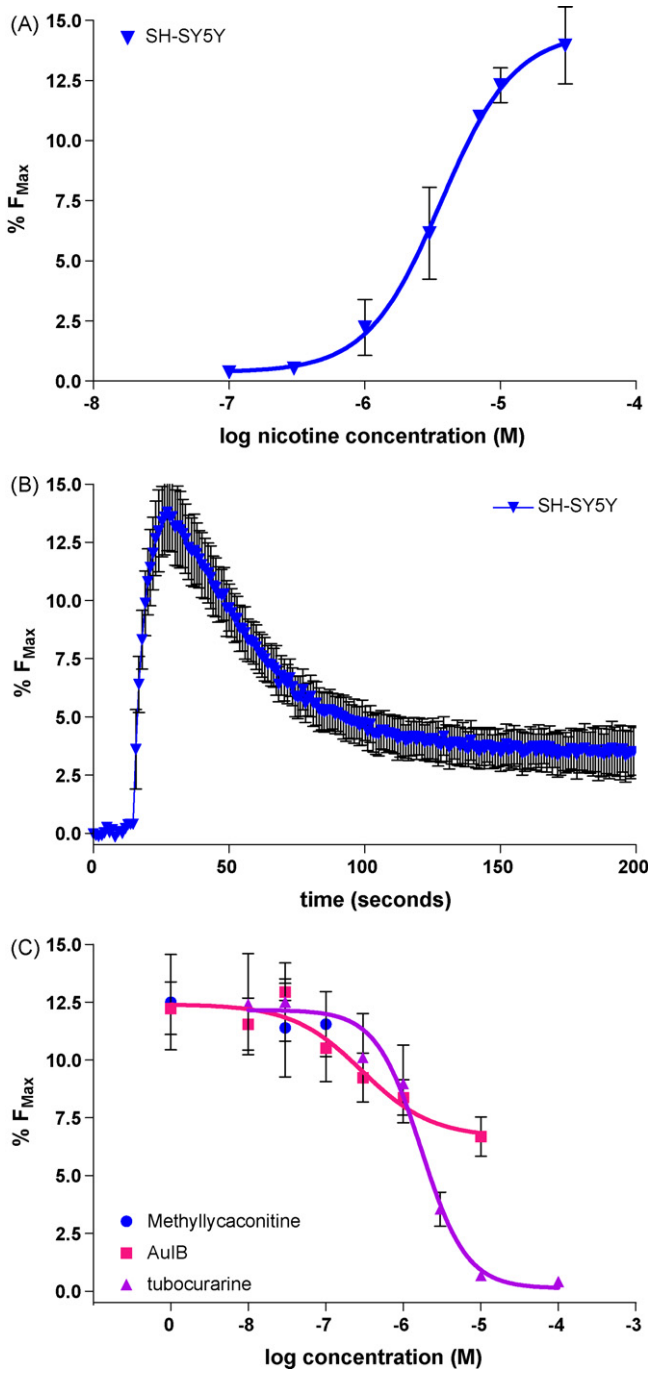

Fig. 4. Nicotine elicits Ca^{2+} responses in SH-SY5Y cells. (A) Concentration–response curve of nicotine-mediated increases in intracellular Ca^{2+} in SH-SY5Y cells. (B) Nicotine-elicited Ca^{2+} responses in SH-SY5Y cells are transient in nature. Shown is a representative response of SH-SY5Y cells to addition of 30 μM nicotine. (C) Ca^{2+} responses in SH-SY5Y cells in response to addition of nicotine are not mediated by the α7 nAChR, as methyllycaconitine (blue) did not inhibit nicotine responses. The α3β4-selective conotoxin AuIB (red) partially inhibited nicotine responses, while tubocurarine (purple) completely and concentration-dependently abolished Ca^{2+} transients elicited by addition of nicotine. Data are presented as mean ± SEM of $n = 3$–4 wells and are representative of 3 independent experiments. (For interpretation of the references to color in this figure legend, the reader is referred to the web version of the article.)

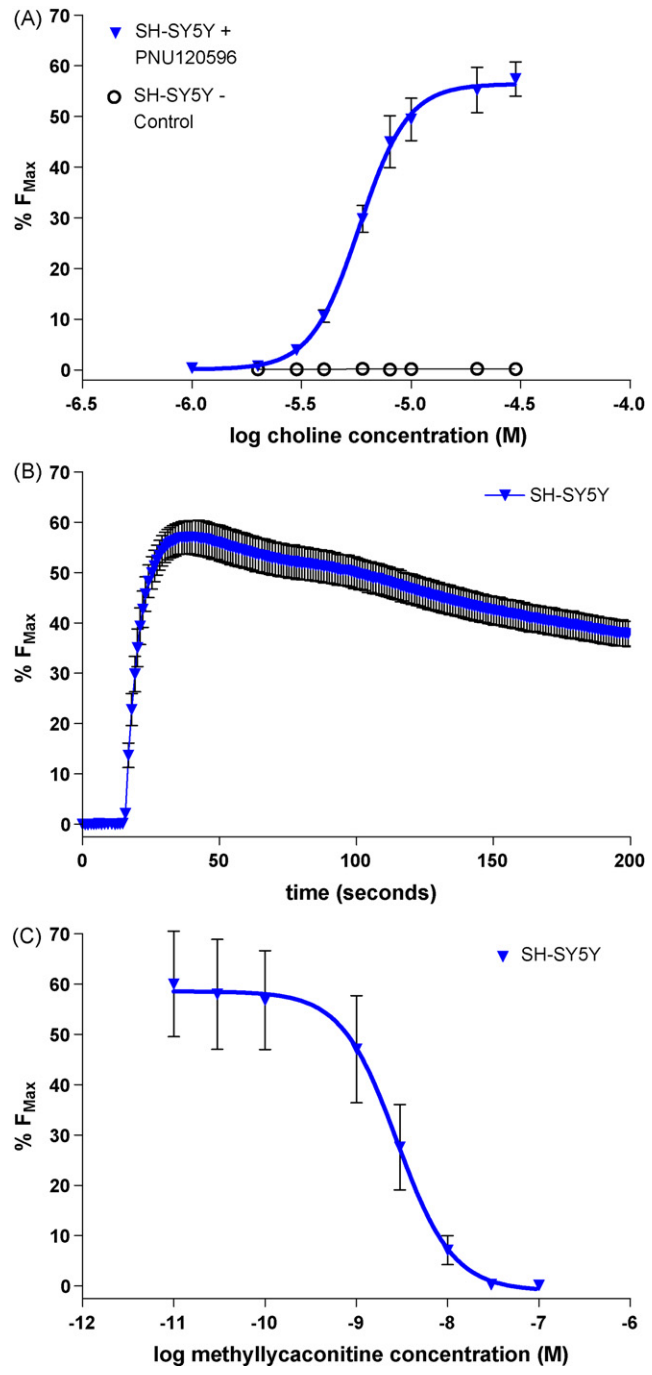

Fig. 5. The α7 nAChR agonist choline elicits Ca^{2+} responses in SH-SY5Y cells in the presence of the α7 nAChR allosteric modulator PNU120596. (A) Addition of the α7 nAChR agonist choline did not cause increases in intracellular Ca^{2+} in SH-SY5Y cells (open circles), however, in the presence of 10 μM PNU120596, an α7-selective allosteric modulator, large concentration-dependent responses in response to choline were observed (blue). (B) Responses to addition of choline were relatively sustained in nature. Shown is a representative Ca^{2+} response to addition of 30 μM choline. (C) Choline-mediated responses were completely and concentration-dependently inhibited by the α7-selective nAChR antagonist methyllycaconitine. Data are presented as mean ± SEM of $n = 3$–4 wells and are representative of 3 independent experiments. (For interpretation of the references to color in this figure legend, the reader is referred to the web version of the article.)

3.6. Neurotensin

Surprisingly, neurotensin only elicited Ca^{2+} transients in HEK293 cells, with an EC_{50} of 6.5×10^{-8} M (Fig. 7A and B). Ca^{2+} responses to addition of neurotensin were small with a maximum response of 2.4 ± 0.9% F_{Max}.

3.7. ATP

HEK293, F11, 50B11 and Neuro2A cells responses to addition of ATP with a transient increase in intracellular Ca^{2+} (Fig. 8A and B). In contrast, ND7/23 and SH-SY5Y cells did not respond to addition of

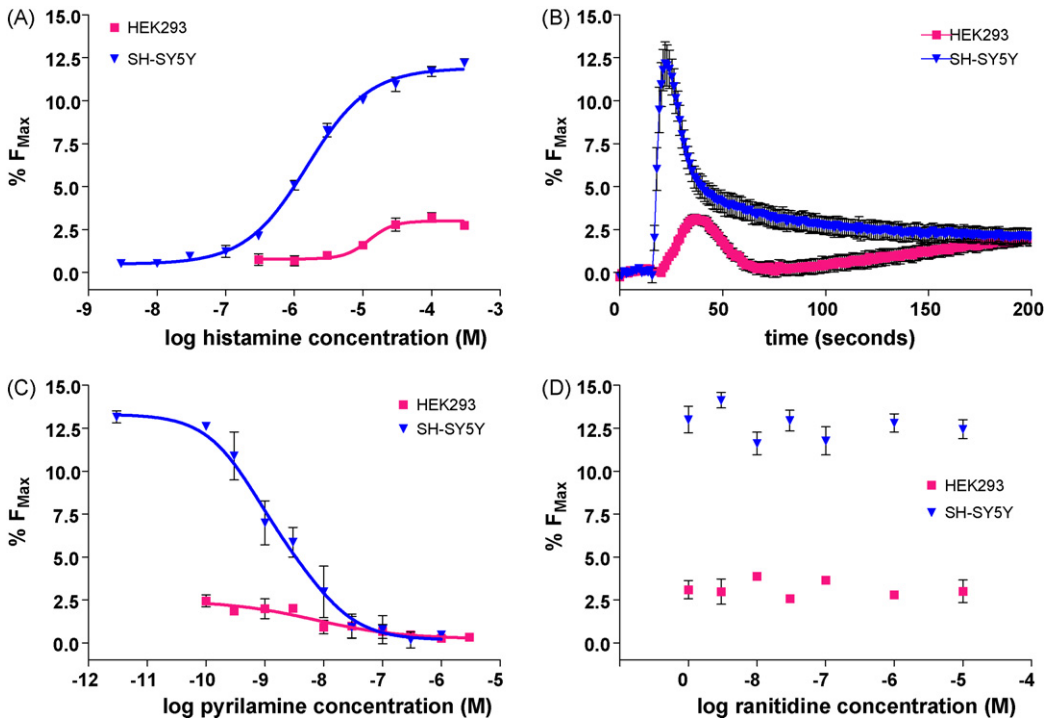

Fig. 6. Histamine causes Ca^{2+} transients in HEK293 and SH-SY5Y cells. (A) Addition of histamine caused concentration-dependent Ca^{2+} transients in HEK293 (red) and SH-SY5Y cells (blue). The magnitude of histamine-elicited responses was significantly larger in SH-SY5Y compared to HEK293 cells. (B) Representative Ca^{2+} transients in response to addition of 100 μM histamine. SH-SY5Y cells responded with rapid increases in intracellular Ca^{2+} that did not return to baseline up to approximately 200 s (blue). HEK293 cells responded with slower increases in Ca^{2+} that returned to baseline within approximately 60 s (red). (C) Histamine-induced Ca^{2+} transients in HEK293 and SH-SY5Y cells are completely and concentration-dependently inhibited by the H1 antagonist pyrilamine, albeit histamine responses in SH-SY5Y cells were significantly more sensitive to inhibition by pyrilamine than in HEK293 cells. (D) The H2-specific antagonist ranitidine did not inhibit Ca^{2+} responses to histamine in HEK293 (red) and SH-SY5Y cells (blue) at concentrations up to 10 μM. Data are presented as mean ± SEM of n = 3–4 wells and are representative of 2–3 independent experiments. (For interpretation of the references to color in this figure legend, the reader is referred to the web version of the article.)

ATP up to 1 mM (data not shown). HEK293 cells exhibited comparatively large responses to ATP and were the most sensitive to ATP-induced Ca^{2+} influx, with an EC_{50} of 9.2×10^{-7} M. In contrast, ATP induced Ca^{2+} responses of intermediate magnitude in F11 cells, with an EC_{50} of 1.3×10^{-5} M, while 50B11 and Neuro2A cells responded with very small increases in intracellular Ca^{2+}, with EC_{50}s of 1.2×10^{-5} and 7.0×10^{-6} M, respectively. Due to the lack of highly selective agonists or antagonists, as well as the large number of ATP-sensitive P2X and P2Y receptors, the exact receptor subtypes contributing to these responses remain to be determined. However, as evidenced by the ability of ATP to elicit Ca^{2+} responses in the absence of extracellular Ca^{2+}, it appears that G-protein coupled P2Y receptors account for the majority of ATP-induced Ca^{2+} influx in HEK293, F11, 50B11 and Neuro2A cells (Fig. 8C–F).

4. Discussion

The study of endogenously expressed receptors and ion channels can provide physiologically relevant information often lacking in over-expression systems which fail to adequately account for the role of auxiliary protein effects on receptor function and regulation. Immortalized neuronal cell lines provide a convenient model to study neuronal pharmacology, circumventing primary culture of neurons, and allowing access to endogenous receptors. However, systematic data on receptors and ion channels expressed in these cell lines is lacking.

Here, we describe the first systematic evaluation of endogenous Ca^{2+} responses to several agonists at potential therapeutic targets in F11, ND7/23, 50B11 as well as Neuro2A, SH-SY5Y and HEK293 cells. These cell lines represent commonly used DRG-derived cells, as well as neuroblastoma cells and a non-neuronal cell line commonly used for expression of neuronal receptors and ion channels. Endogenous Ca^{2+} responses were obtained upon addition of bradykinin, trypsin, ATP, nicotine, acetylcholine, histamine and neurotensin in one or more of these cell lines. While precise involvement of specific receptor subtypes remains to be verified at protein and mRNA level, insight into possible receptor subtypes involved in these responses was provided by establishment of full concentration–response curves as well as pharmacological characterization using receptor subtype specific agonists and antagonists. Such information is particularly valuable when identifying cell lines which are suitable to study putative neuronal targets, as over-expression of these targets in non-neuronal cell lines may alter the properties of these receptors and ion channels. For example, TRPV1 overexpressed in non-neuronal cell lines has a markedly different pharmacological profile compared to native TRPV1, most likely due to the absence of the neuronal accessory protein Fas-associated factor 1 [51]. In addition, the reverse is true when expressing receptors in cell lines that already constitutively express the target of interest. One such example is the bradykinin B2 receptor, which, despite being endogenously expressed in HEK293 cells, has been overexpressed in these cells to study bradykinin signaling [52,53]. Not surprisingly, this can lead to results that are conflicting or difficult to interpret, especially when non-human receptor is expressed. This systematic characterization of receptors endogenously expressed in commonly used cell lines may facilitate the study of receptors and ion channels associated with neuronal signaling.

4.1. Trypsin

Trypsin activates protease-activated receptors or PARs, which are GPCR that couple to increases in intracellular Ca^{2+} through activation of PLC (phospholipase C). Specifically, trypsin activates

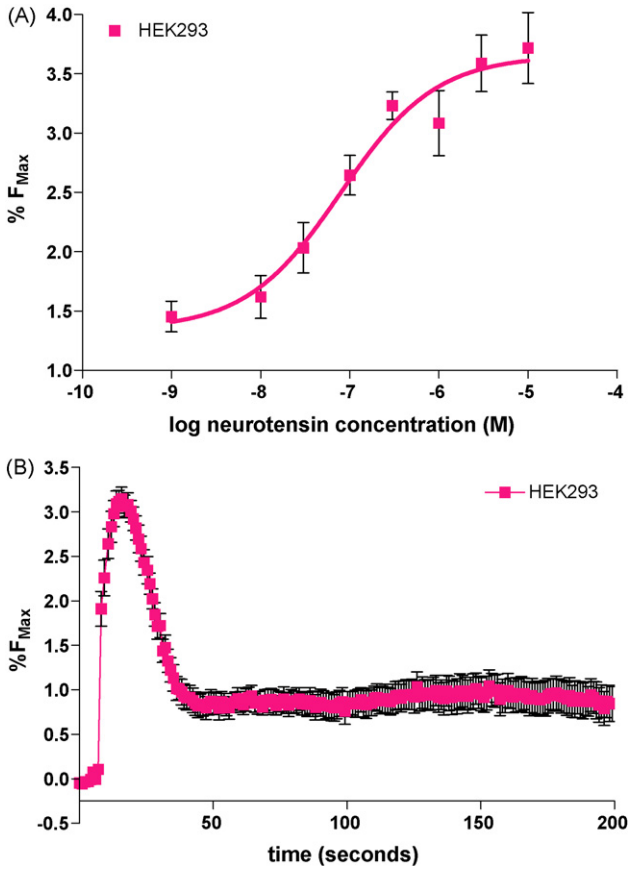

Fig. 7. Neurotensin causes Ca^{2+} transients in HEK293 cells. (A) Addition of neurotensin caused small but concentration-dependent increases in intracellular Ca^{2+} in HEK293, but not any of the neuronal cell lines tested. (B) Representative Ca^{2+} transient caused by addition of 100 nM neurotensin in HEK293 cells. Data are presented as mean ± SEM of n = 6–8 wells and are representative of 3 independent experiments.

PAR2 with an EC_{50} of approximately 1–10 nM [54–56], but also PAR1 and PAR4 isoforms albeit with higher EC_{50}s [57,58]. Surprisingly, all cell lines except 50B11 and ND7/23 responded to addition of trypsin with increases in intracellular Ca^{2+}, though the higher EC_{50} values suggest the involvement of PAR isoforms other than PAR2 in these neuronal cell lines. In light of expression of PAR1 and PAR4 on both central and peripheral neurons, involvement of one or more of these isoforms in the trypsin-mediated responses in F11, SH-SY5Y and Neuro2A cells seems likely. In contrast, PAR2 expression has previously been reported in HEK293 cells [59] and indeed the EC_{50} of trypsin-mediated Ca^{2+} mobilization was consistent with activation of PAR2. Surprisingly, trypsin at an EC_{50} concentration (10 nM) induced Ca^{2+} oscillations in HEK293 cells, similar to thrombin-evoked responses in platelets [60]. As this is the first report to describe trypsin-induced Ca^{2+} oscillations, the physiological mechanism involved remains to be determined, though it is likely that release of Ca^{2+} from intracellular stores contributes to this phenomenon. It has recently been proposed that the release of Ca^{2+}, and thus Ca^{2+} oscillations, is controlled by the regulators of G protein signaling (RGS) proteins, in particular RGS4, which in turn is regulated by PIP_3 and Ca^{2+}-calmodulin [61,62]. It remains to be determined if such a mechanism could also contribute to the trypsin-evoked oscillations observed in here in HEK293 cells.

4.2. Bradykinin

Bradykinin B1 and B2 receptors belong to a GPCR family that signals through G_q to increases in intracellular Ca^{2+}. The principal agonist of these receptors is bradykinin, which activates recombinant human B1 with an EC_{50} of 1 μM and B2 with an EC_{50} of 2 nM [63]. However, while the bradykinin B2 receptor is constitutively expressed in many tissues, including the central and peripheral nervous system, bradykinin B1 receptor expression is rapidly induced from low basal levels following tissue injury and inflammation [15,64]. Accordingly, bradykinin B2 receptors may play a greater role in acute pain, whereas bradykinin B1 receptors appear an interesting therapeutic target in chronic pain [15,64]. Interestingly, F11 cells responded to addition of nM and sub-nanomolar concentrations of bradykinin with Ca^{2+} transients that were best fitted with a two-site model. Heterogeneity of B2 receptors has been suggested previously, with high and low affinity bradykinin B2 receptor sites observed in several tissues [65–68]. A related phenomenon has been described in NG108 neuroblastoma cells [67], where guanyl-5′-yl-imidodiphosphate converted the high affinity bradykinin B2 site into a low affinity site. However, such a mechanism is not necessarily applicable to functional responses in live cells and the different affinities of bradykinin observed in F11 cells may represent different B2 receptor subtypes, binding to non-bradykinin receptor sites, or may perhaps be the result of activation of different effector pathways or cell sub-populations. While SH-SY5Y and Neuro2A cells responded only to high concentrations of bradykinin and ND7/23 cells responded to nM concentrations of bradykinin, which could suggest a B1 response, inhibition of bradykinin responses by the B2 antagonist HOE-140 supports predominant involvement of B2 receptors in all three cell lines.

4.3. Acetylcholine and nicotine

Acetylcholine activates muscarinic and nicotinic AChR, of which there are several subtypes. HEK293 and SH-SY5Y cells responded to addition of acetylcholine, while only SH-SY5Y cells responded to nicotine, suggesting that acetylcholine-induced Ca^{2+} responses in HEK293 cells are mediated by muscarinic rather than nicotinic receptors. Indeed, HEK293 cells express M3 muscarinic AChR [50], though the presence of M1 muscarinic receptors has also been suggested [69,70]. Acetylcholine responses in HEK293 cells displayed a marked second phase, indicative of M3 rather than M1 acetylcholine receptor Ca^{2+} mobilization characteristics [71]. Supporting the predominant involvement of M3 receptors in the acetylcholine-evoked response in HEK293 cells, the M3-specific antagonist *p*-fluorohexahydro-sila-difenidol hydrochloride completely abolished acetylcholine-induced Ca^{2+} transients.

Although the presence of α7 and α5 nicotinic AChR subunits in HEK293 cells has been suggested at the mRNA level [72], neither nicotine nor the α7-selective agonist choline were able to evoke Ca^{2+} responses in HEK293 cells. Indeed, this is consistent with the reported absence of α7 AChR protein endogenously expressed in HEK293 cells [73]. Conversely, SH-SY5Y cells have been reported to express α3, α5, α7, β2 and β4 nicotinic AChR subunits [74,75] and did indeed respond to addition of nicotine with transient increases in intracellular Ca^{2+}. These responses were not mediated through α7 nicotinic AChR, as the specific α7 antagonist methyllycaconitine did not inhibit nicotine-evoked responses. However, SH-SY5Y neuroblastoma cells do express functional α7 nAChR, as responses to the specific α7 agonists choline in the presence of the α7 allosteric modulator PNU120596 were completely abolished by methyllycaconitine. Consistent with a model describing >1 agonist binding sites in the homopentameric α7 nAChR, the Hill slope for choline-induced responses was approximately 2.7 ± 0.3, suggesting that >1 molecule of choline is required for activation of α7 nAChR, while block of only one binding site by methyllycaconitine is sufficient to completely abolish these responses. Nicotine-evoked responses were inhibited by tubocurarine with an IC_{50} of

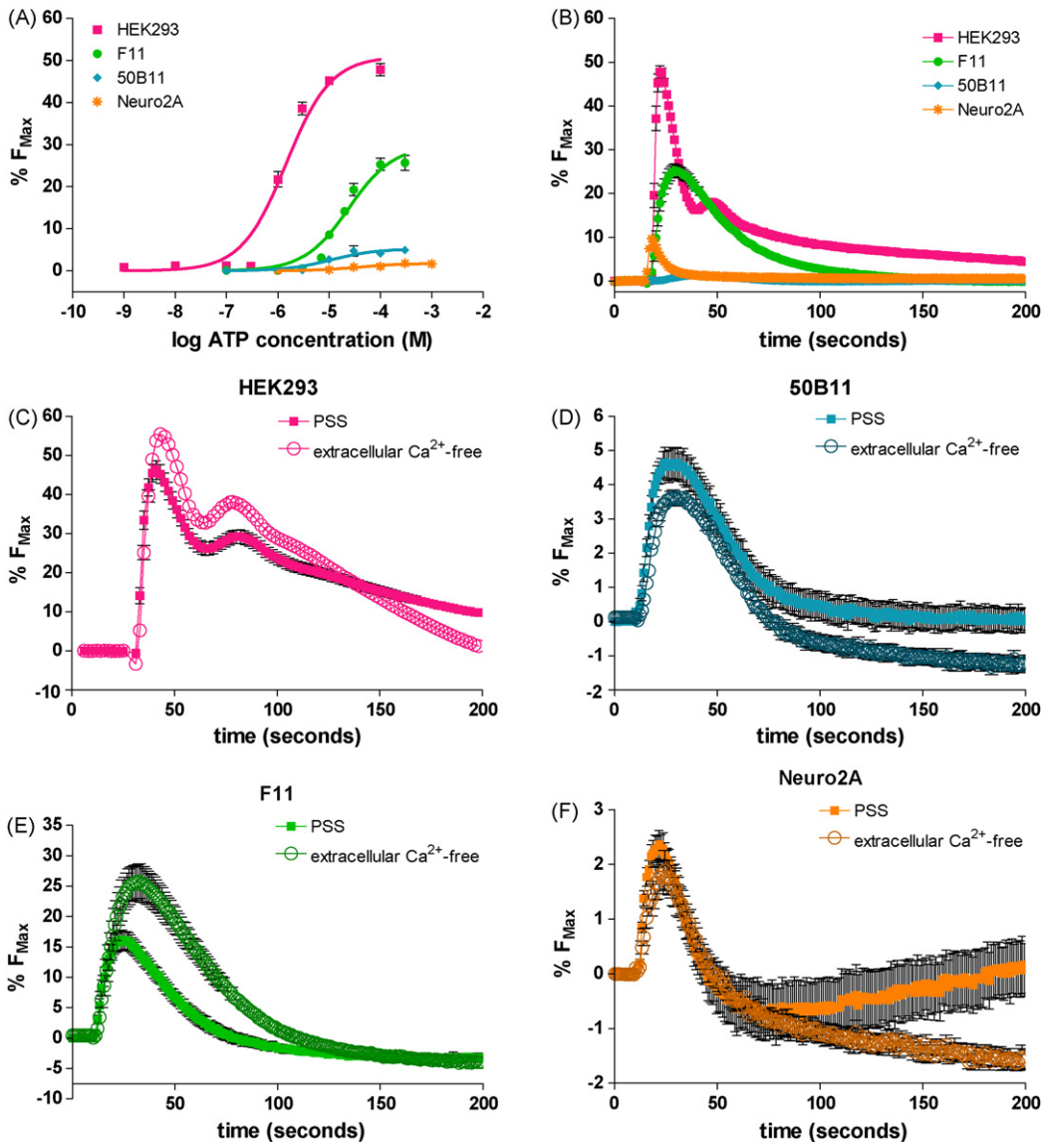

Fig. 8. ATP induces Ca^{2+} responses in HEK293, F11, 50B11 and Neuro2A cells. (A) Addition of ATP concentration-dependently increased intracellular Ca^{2+} in HEK293 (red), F11 (green), 50B11 (turquoise) and Neuro2A (orange) cells, but not in ND7/23 or SH-SY5Y cells. The magnitude of ATP-induced responses was largest in HEK293 cells, intermediate in F11 and comparatively small in 50B11 and Neuro2A cells. (B) Representative Ca^{2+} responses to addition of 100 μM ATP in HEK293 (red), F11 (green), 50B11 (turquoise) and Neuro2A (orange) cells. ATP-mediated responses were transient in nature, with a biphasic response evident in HEK293 cells. (C–F) ATP-mediated increases in intracellular Ca^{2+} in the presence (PSS, filled symbols) and absence (extracellular Ca^{2+}-free, open symbols) of extracellular Ca^{2+}. Ca^{2+} transients in response to ATP were not significantly inhibited by the absence of extracellular Ca^{2+} in HEK293 (C), 50B11 (D), F11 (E) and Neuro2A (F) cells, suggesting contribution of P2Y receptors to the ATP response. Data are presented as mean ± SEM of $n = 3$–4 wells and are representative of 3 independent experiments. (For interpretation of the references to color in this figure legend, the reader is referred to the web version of the article.)

1.7×10^{-6} M, suggesting involvement of nicotinic AChR containing β2 subunits [76]. While previous studies were unable to demonstrate contribution of α3β4 nAChR to the nicotine-evoked Ca^{2+} responses in SH-SY5Y cells [75], we found that the α3β4-specific conotoxin AuIB [77] inhibited approximately 50% of the nicotine-evoked response, confirming involvement of α3β4 containing nAChRs. Surprisingly, the acetylcholine-evoked response was also completely abolished by the M3 antagonist *p*-fluorohexahydro-sila-difenidol hydrochloride, suggesting that activation of nicotinic receptor subtypes did not contribute to the acetylcholine response in SH-SY5Y cells.

4.4. Histamine

All four subtypes of histamine receptors, H1–H4, belong to the GPCR family of receptors, with H1 linked to intracellular Ca^{2+} mobilization through G_q coupled IP3 production and subsequent store release. Albeit histamine H2, H3 and H4 receptors are generally considered to couple to other G protein effectors including adenylate cyclase and voltage-gated Ca^{2+} channels, several reports have demonstrated increases in intracellular Ca^{2+} through activation of H4, H2 and H3 receptors in mast cells, keratinocytes and neuroblastoma cells, respectively [78–80]. However, where histamine H1 and H2 subtypes demonstrate relatively low affinity to histamine (EC_{50}s of 24 and ~10 μM, respectively) [81,82], H3 and H4 receptors are high affinity histamine receptors with EC_{50} values in the nanomolar range [83,84].

In light of the relatively wide tissue distribution of histamine H1 and H2 receptors, together with literature EC_{50} values similar to those obtained in the present study, it seems likely that the histamine-mediated increase in Ca^{2+} observed in HEK293 and SH-SY5Y cells are mediated through H1 or H2 receptors. Indeed, using

the H1 antagonist pyrilamine, we were able to show that the histamine-induced responses in HEK293 cells were mediated through H1 receptors, with responses completely inhibited by pyrilamine. Indeed, the H2-specific antagonist ranitidine had no effect on histamine-induced responses, confirming predominant involvement of H1 receptors. A second, low affinity histamine site was apparent in some batches of SH-SY5Y cells. While a model suggesting two binding states of the H1 receptor has indeed been proposed in rat thalamus and guinea-pig cardiac muscle [85,86], such a mechanism is not necessarily applicable to functional responses in live cells, and the precise causes of the second site remain to be determined. These results are in contrast to the reported absence of endogenous histamine H1 receptor mRNA in HEK293 cells [72] or lack of any report on histamine receptor expression in SH-SY5Y cells. Both HEK293 and SH-SY5Y cells could be useful to further study the pharmacology of endogenously expressed human histamine receptors.

4.5. Neurotensin

The neuropeptide neurotensin exerts its various central and peripheral biological roles through activation of the neurotensin receptors NTS1, NTS2 and NTS3 [87]. While NTS3 is homologous to gp95/sortilin, NTS1 and NTS2 are GPCRs which act via activation of PLC pathways linked to increases in intracellular Ca^{2+}. Surprisingly, HEK293 cells responded to addition of neurotensin with transient increases in intracellular Ca^{2+}, suggesting the presence of functional NTS1 or NTS2 receptors. HEK293 cells have been reported to be derived from transformation of neuronal lineage cells in embryonic kidney cultures and display several properties of neuronal cells [72]. Specifically, HEK293 cells are reported to express neuronal proteins such as neurofilament subunits usually restricted to expression in neuronal cells, and many of the intracellular signaling pathways and membrane proteins restricted to neuronal cells, including voltage-gated Ca^{2+} and potassium channels, are also present in HEK cells [72,88].

Neurotensin has also been reported to activate bradykinin B2 receptors in PC12 cells, albeit at high μM EC_{50} [89]. However, it is unlikely that neurotensin-evoked Ca^{2+} transients in HEK293 cells were mediated through activation of bradykinin B2 receptors, as functional bradykinin receptors were expressed in all other cell lines except 50B11 cells, but neurotensin did not evoke responses in any of these cell lines. In addition, the observed EC_{50} for neurotensin-evoked Ca^{2+} responses was 7.9×10^{-8} M, considerably lower than those reported to be required for activation of B2 receptors by neurotensin. Thus, it appears that HEK293 cells express endogenous neurotensin receptors, further supporting the neuronal-like character of a cell line often considered to be of kidney epithelial origin. While the precise neurotensin receptor subtypes involved in mediating neurotensin-evoked Ca^{2+} responses in HEK cells remain to be determined, the high affinity NTS1 appears the most likely candidate, as activation of NTS2 by neurotensin does not lead to an increase in Ca^{2+} in overexpressed systems [90].

4.6. ATP

Several subtypes of purinergic receptors can respond to addition of ATP with increases in intracellular Ca^{2+}. Broadly, these receptors include the ligand-gated ion channels P2X1 to P2X7 and the GPCRs P2Y2, P2Y4, P2Y11 and P2Y12. Not surprisingly, due to the wide tissue distribution of these receptors, most cell lines assessed here responded to addition of ATP with increases in intracellular Ca^{2+}, albeit the magnitude of responses varied widely. Interestingly, no significant increases in intracellular Ca^{2+} were apparent upon addition of 1 mM ATP in ND7/23 and SH-SY5Y cells. While the presence of P2X7 receptors in SH-SY5Y cells has been reported previously and these cells respond with increases in intracellular Ca^{2+} to BzATP [91], it is possible that we did not observe P2X7 responses here because the response to ATP is either absent or undetectable. Due to the lack of highly selective pharmacological modulators of purinergic receptors, assessment of the precise receptor subtypes involved in these responses is beyond the scope of this study. However, the ability of ATP to elicit Ca^{2+} responses in the absence of extracellular Ca^{2+} would suggest predominant involvement of P2Y rather than P2X receptors in HEK, Neuro2A, F11 and 50B11 cells.

While several agonists did not produce Ca^{2+} responses, this does not necessarily indicate the absence of functional receptors, but rather the lack of coupling to intracellular Ca^{2+} pathways. Endogenous β2 adrenergic receptors are reported to be expressed in HEK cells, however, as these receptors do not couple to G_q, no Ca^{2+} signal was observed in response to addition of noradrenaline [92]. Furthermore, the absence of a noradrenaline response is informative as it suggests the absence of α adrenoreceptors, which are known to couple to increases in intracellular Ca^{2+}. Similarly, the presence of glutamate receptors, specifically mGlu1, has been described at mRNA level, suggesting that HEK293 cells should respond with increases in intracellular Ca^{2+} to addition of glutamate [72,93]. Absence of a Ca^{2+} response could indicate insufficient expression of functional protein, and indeed, the absence of endogenous mGlu1 responses in HEK293 cells has been reported previously [94].

The responses described here (with the exception of histamine responses in SH-SY5Y cells) were robust over several months and multiple passages. Surprisingly, although TRPV1 expression has been reported in F11 and 50B11 cells [42,95], none of the cell lines assessed here responded to addition of the TRPV1 agonist capsaicin with increases in intracellular Ca^{2+}. While the causality of these differences is not entirely clear, the absence of TRPV1 responses in F11 cells has previously been attributed to batch-specific variation which could be a contributing factor here. In addition, Ca^{2+} responses to addition of capsaicin were previously observed at relatively high capsaicin (10 μM) concentration and may have involved non-specific Ca^{2+} increases. Alternatively, variations in experimental or differentiation conditions may also contribute to these differences.

In conclusion, this is the first study to establish full concentration–response curves to trypsin, bradykinin, acetylcholine, nicotine, choline, histamine, neurotensin and ATP, enabling direct comparison of the magnitude, potency and kinetics of their effect across HEK293, SH-SY5Y, Neuro2A, 50B11, ND7/23 and F11 cells. In the course of these studies we identified a surprising Ca^{2+} transient in response to neurotensin and Ca^{2+} oscillations in response to trypsin in HEK293 cells; a high affinity bradykinin effect in F11 cells; and an unexpected lack of responses to ATP in SH-SY5Y and ND7/23 cells. Possible receptor subtype(s) involved in these responses were inferred from agonist EC_{50} values, in conjunction with IC_{50} values of receptor subtype selective antagonists where possible. Systematic characterization of endogenous Ca^{2+} responses in cell lines of human origin, in particular HEK293 and SH-SY5Y cells, provide access to endogenously expressed human receptors, presumably expressed together with the appropriate accessory proteins and signaling machinery intact, which may facilitate the discovery and characterization of therapeutics acting at these targets. The absence of calcium signaling in response to agonists of targets commonly found in DRG neurons in the DRG-derived cell lines F11, 50B11 and ND7/23 suggests that these cells lines are representative of a subset of DRG cells that do not express common nociceptors or do not utilize the same signaling pathways as native DRG neurons which typically respond with increases in intracellular Ca^{2+} to the agonists

investigated. Additional immortalized DRG cell lines selected for expression of markers such as CGRP (calcitonin-gene related peptide) or IB4 (isolectin B4) that respond to other agonists of antinociceptive targets not covered by the cell lines assessed here (such as adenosine, capsaicin, dopamine, GABA, glutamate, morphine, neurokinin A and B, NMSA, noradrenaline, serotonin and substance P) may expand the range of endogenously expressed nociceptive targets accessible with this approach.

Conflict of interest

The authors declare no competing interest.

Acknowledgements

This work was supported by a NHMRC Australian Based Biomedical Post doctorate Fellowship (IV) and an NHMRC Program Grant (RJL). RJL is an NHMRC Research Fellow.

Contributions: IV carried out experimental work and drafted the manuscript, RJL participated in the study design and coordination and helped to draft the manuscript. All authors read and approved the final manuscript.

References

[1] Raggenbass M, Bertrand D. Nicotinic receptors in circuit excitability and epilepsy. J Neurobiol 2002;53:580–9.
[2] Khosravani H, Zamponi GW. Voltage-gated calcium channels and idiopathic generalized epilepsies. Physiol Rev 2006;86:941–66.
[3] Dray A. Neuropathic pain: emerging treatments. Br J Anaesth 2008;101:48–58.
[4] Jensen AA, Frolund B, Liljefors T, Krogsgaard-Larsen P. Neuronal nicotinic acetylcholine receptors: structural revelations, target identifications, and therapeutic inspirations. J Med Chem 2005;48:4705–45.
[5] Triggle DJ. Drug targets in the voltage-gated calcium channel family: why some are and some are not. Assay Drug Dev Technol 2003;1:719–33.
[6] Lu Y, Wang X. Genes associated with idiopathic epilepsies: a current overview. Neurol Res 2009;31:135–43.
[7] Bowie D. Ionotropic glutamate receptors & CNS disorders. CNS Neurol Disord Drug Targets 2008;7:129–43.
[8] Saito T, Bunnett NW. Protease-activated receptors: regulation of neuronal function. Neuromolecular Med 2005;7:79–99.
[9] Vergnolle N, Wallace JL, Bunnett NW, Hollenberg MD. Protease-activated receptors in inflammation, neuronal signaling and pain. Trends Pharmacol Sci 2001;22:146–52.
[10] Asfaha S, Cenac N, Houle S, Altier C, Papez MD, Nguyen C, et al. Protease-activated receptor-4: a novel mechanism of inflammatory pain modulation. Br J Pharmacol 2007;150:176–85.
[11] Oliver KR, Hill RG. Feeling below PAR: proteinase-activated receptors and the perception of neuroinflammatory pain. Pharmacogenomics J 2002;2:10–1.
[12] Bueno L. Protease activated receptor 2: a new target for IBS treatment. Eur Rev Med Pharmacol Sci 2008;12(Suppl. 1):95–102.
[13] Lohman RJ, O'Brien TJ, Cocks TM. Protease-activated receptor-2 regulates trypsin expression in the brain and protects against seizures and epileptogenesis. Neurobiol Dis 2008;30:84–93.
[14] Meini S, Maggi CA. Knee osteoarthritis: a role for bradykinin? Inflamm Res 2008;57:351–61.
[15] Chen JJ, Johnson EJ. Targeting the bradykinin B1 receptor to reduce pain. Expert Opin Ther Targets 2007;11:21–35.
[16] Kitabgi P. Targeting neurotensin receptors with agonists and antagonists for therapeutic purposes. Curr Opin Drug Discov Devel 2002;5:764–76.
[17] Allen JW, Hofer K, McCumber D, Wagstaff JD, Layer RT, McCabe RT, et al. An assessment of the antinociceptive efficacy of intrathecal and epidural contulakin-G in rats and dogs. Anesth Analg 2007;104:1505–13. table of contents.
[18] Lee HK, Zhang L, Smith MD, White HS, Bulaj G. Glycosylated neurotensin analogues exhibit sub-picomolar anticonvulsant potency in a pharmacoresistant model of epilepsy. ChemMedChem 2009;4:400–5.
[19] Kinkead B, Nemeroff CB. Novel treatments of schizophrenia: targeting the neurotensin system. CNS Neurol Disord Drug Targets 2006;5:205–18.
[20] Wein AJ. Muscarinic acetylcholine receptor knockout mice: novel phenotypes and clinical implications. J Urol 2005;173:2199.
[21] Wess J. Muscarinic acetylcholine receptor knockout mice: novel phenotypes and clinical implications. Annu Rev Pharmacol Toxicol 2004;44:423–50.
[22] Tata AM. Muscarinic acetylcholine receptors: new potential therapeutic targets in antinociception and in cancer therapy. Recent Pat CNS Drug Discov 2008;3:94–103.
[23] Wess J, Duttaroy A, Gomeza J, Zhang W, Yamada M, Felder CC, et al. Muscarinic receptor subtypes mediating central and peripheral antinociception studied with muscarinic receptor knockout mice: a review. Life Sci 2003;72:2047–54.
[24] Bozzi Y, Borrelli E. Dopamine in neurotoxicity and neuroprotection: what do D2 receptors have to do with it? Trends Neurosci 2006;29:167–74.
[25] Wood PB. Role of central dopamine in pain and analgesia. Expert Rev Neurother 2008;8:781–97.
[26] Raffa RB. Antihistamines as analgesics. J Clin Pharm Ther 2001;26:81–5.
[27] Gemkow MJ, Davenport AJ, Harich S, Ellenbroek BA, Cesura A, Hallett D. The histamine H3 receptor as a therapeutic drug target for CNS disorders. Drug Discov Today 2009;14:509–15.
[28] Tang FR, Bradford HF, Ling EA. Metabotropic glutamate receptors in the control of neuronal activity and as targets for development of anti-epileptogenic drugs. Curr Med Chem 2009;16:2189–204.
[29] Neugebauer V. Metabotropic glutamate receptors—important modulators of nociception and pain behavior. Pain 2002;98:1–8.
[30] Enna SJ, McCarson KE. The role of GABA in the mediation and perception of pain. Adv Pharmacol 2006;54:1–27.
[31] Bagdy G, Kecskemeti V, Riba P, Jakus R. Serotonin and epilepsy. J Neurochem 2007;100:857–73.
[32] Sommer C. Serotonin in pain and analgesia: actions in the periphery. Mol Neurobiol 2004;30:117–25.
[33] Okamoto K, Imbe H, Morikawa Y, Itoh M, Sekimoto M, Nemoto K, et al. 5-HT2A receptor subtype in the peripheral branch of sensory fibers is involved in the potentiation of inflammatory pain in rats. Pain 2002;99:133–43.
[34] Wu S, Zhu M, Wang W, Wang Y, Li Y, Yew DT. Changes of the expression of 5-HT receptor subtype mRNAs in rat dorsal root ganglion by complete Freund's adjuvant-induced inflammation. Neurosci Lett 2001;307:183–6.
[35] Burnstock G. Purinergic signalling and disorders of the central nervous system. Nat Rev Drug Discov 2008;7:575–90.
[36] Yoon MH, Bae HB, Choi JI, Kim SJ, Chung ST, Kim CM. Roles of adenosine receptor subtypes in the antinociceptive effect of intrathecal adenosine in a rat formalin test. Pharmacology 2006;78:21–6.
[37] Liu XJ, Salter MW. Purines and pain mechanisms: recent developments. Curr Opin Investig Drugs 2005;6:65–75.
[38] Donnelly-Roberts D, McGaraughty S, Shieh CC, Honore P, Jarvis MF. Painful purinergic receptors. J Pharmacol Exp Ther 2008;324:409–15.
[39] Reeve AJ, Dickenson AH. The roles of spinal adenosine receptors in the control of acute and more persistent nociceptive responses of dorsal horn neurones in the anaesthetized rat. Br J Pharmacol 1995;116:2221–8.
[40] Platika D, Baizer L, Fishman MC. Sensory neurons "immortalized" by fusion with neuroblastoma cells. Trans Assoc Am Physicians 1985;98:301–4.
[41] Wood JN, Bevan SJ, Coote PR, Dunn PM, Harmar A, Hogan P, et al. Novel cell lines display properties of nociceptive sensory neurons. Proc Biol Sci 1990;241:187–94.
[42] Chen W, Mi R, Haughey N, Oz M, Hoke A. Immortalization and characterization of a nociceptive dorsal root ganglion sensory neuronal line. J Peripher Nerv Syst 2007;12:121–30.
[43] Biedler JL, Helson L, Spengler BA. Morphology and growth, tumorigenicity, and cytogenetics of human neuroblastoma cells in continuous culture. Cancer Res 1973;33:2643–52.
[44] Olmsted JB, Carlson K, Klebe R, Ruddle F, Rosenbaum J. Isolation of microtubule protein from cultured mouse neuroblastoma cells. Proc Natl Acad Sci USA 1970;65:129–36.
[45] Graham FL, Smiley J, Russell WC, Nairn R. Characteristics of a human cell line transformed by DNA from human adenovirus type 5. J Gen Virol 1977;36:59–74.
[46] Mutschler E, Moser U, Wess J, Lambrecht G. Muscarinic receptor subtypes—pharmacological, molecular biological and therapeutical aspects. Pharm Acta Helv 1995;69:243–58.
[47] Zlotos DP, Bender W, Holzgrabe U. Muscarinic receptor agonists and antagonists. Expert Opin Ther Patents 1999;9:1029–53.
[48] Weill C, Galzi JL, Chasserot-Golaz S, Goeldner M, Ilien B. Functional characterization and potential applications for enhanced green fluorescent protein- and epitope-fused human M1 muscarinic receptors. J Neurochem 1999;73:791–801.
[49] Alexander SP, Mathie A, Peters JA. Guide to receptors and channels (GRAC), 2nd edition. Br J Pharmacol 2006;147(Suppl. 3):S1–68.
[50] Dowling MR, Willets JM, Budd DC, Charlton SJ, Nahorski SR, Challiss RA. A single point mutation (N514Y) in the human M3 muscarinic acetylcholine receptor reveals differences in the properties of antagonists: evidence for differential inverse agonism. J Pharmacol Exp Ther 2006;317:1134–42.
[51] Kim S, Kang C, Shin CY, Hwang SW, Yang YD, Shim WS, et al. TRPV1 recapitulates native capsaicin receptor in sensory neurons in association with Fas-associated factor 1. J Neurosci 2006;26:2403–12.
[52] Pizard A, Blaukat A, Muller-Esterl W, Alhenc-Gelas F, Rajerison RM. Bradykinin-induced internalization of the human B2 receptor requires phosphorylation of three serine and two threonine residues at its carboxyl tail. J Biol Chem 1999;274:12738–47.
[53] Lamb ME, De Weerd WF, Leeb-Lundberg LM. Agonist-promoted trafficking of human bradykinin receptors: arrestin- and dynamin-independent sequestration of the B2 receptor and bradykinin in HEK293 cells. Biochem J 2001;355:741–50.
[54] Luo W, Wang Y, Reiser G. Two types of protease-activated receptors (PAR-1 and PAR-2) mediate calcium signaling in rat retinal ganglion cells RGC-5. Brain Res 2005;1047:159–67.
[55] Shpacovitch VM, Brzoska T, Buddenkotte J, Stroh C, Sommerhoff CP, Ansel JC, et al. Agonists of proteinase-activated receptor 2 induce cytokine release and

activation of nuclear transcription factor kappaB in human dermal microvascular endothelial cells. J Invest Dermatol 2002;118:380–5.
[56] Steinhoff M, Vergnolle N, Young SH, Tognetto M, Amadesi S, Ennes HS, et al. Agonists of proteinase-activated receptor 2 induce inflammation by a neurogenic mechanism. Nat Med 2000;6:151–8.
[57] Xu WF, Andersen H, Whitmore TE, Presnell SR, Yee DP, Ching A, et al. Cloning and characterization of human protease-activated receptor 4. Proc Natl Acad Sci USA 1998;95:6642–6.
[58] Blackhart BD, Emilsson K, Nguyen D, Teng W, Martelli AJ, Nystedt S, et al. Ligand cross-reactivity within the protease-activated receptor family. J Biol Chem 1996;271:16466–71.
[59] Grishina Z, Ostrowska E, Halangk W, Sahin-Toth M, Reiser G. Activity of recombinant trypsin isoforms on human proteinase-activated receptors (PAR): mesotrypsin cannot activate epithelial PAR-1, -2, but weakly activates brain PAR-1. Br J Pharmacol 2005;146:990–9.
[60] Ozaki Y, Yatomi Y, Wakasugi S, Shirasawa Y, Saito H, Kume S. Thrombin-induced calcium oscillation in human platelets and MEG-01, a megakaryoblastic leukemia cell line. Biochem Biophys Res Commun 1992;183:864–71.
[61] Shin DM, Luo X, Wilkie TM, Miller LJ, Peck AB, Humphreys-Beher MG, et al. Polarized expression of G protein-coupled receptors and an all-or-none discharge of Ca^{2+} pools at initiation sites of $[Ca^{2+}]i$ waves in polarized exocrine cells. J Biol Chem 2001;276:44146–5.
[62] Luo X, Popov S, Bera AK, Wilkie TM, Muallem S. RGS proteins provide biochemical control of agonist-evoked $[Ca^{2+}]i$ oscillations. Mol Cell 2001; 7:651–60.
[63] Simpson PB, Woollacott AJ, Hill RG, Seabrook GR. Functional characterization of bradykinin analogues on recombinant human bradykinin B(1) and B(2) receptors. Eur J Pharmacol 2000;392:1–9.
[64] Marceau F, Regoli D. Bradykinin receptor ligands: therapeutic perspectives. Nat Rev Drug Discov 2004;3:845–52.
[65] Reissmann S, Pagelow I, Liebmann C, Steinmetzger H, Jankova T, Arold H. Investigations on the mechanism of bradykinin action on smooth muscles. In: Papasova MA, editor. Physiology and Pharmacology of Smooth Muscle. Sofia: Bulgarian Academy of Science; 1977. pp. 208–17.
[66] Odya CE, Goodfriend TL, Pena C. Bradykinin receptor-like binding studied with iodinated analogues. Biochem Pharmacol 1980;29:175–85.
[67] Hall JM. Bradykinin receptors: pharmacological properties and biological roles. Pharmacol Ther 1992;56:131–90.
[68] Osugi T, Imaizumi T, Mizushima A, Uchida S, Yoshida H. Phorbol ester inhibits bradykinin-stimulated inositol trisphosphate formation and calcium mobilization in neuroblastoma × glioma hybrid NG108-15 cells. J Pharmacol Exp Ther 1987;240:617–22.
[69] Conklin BR, Chabre O, Wong YH, Federman AD, Bourne HR. Recombinant Gq alpha. Mutational activation and coupling to receptors and phospholipase C. J Biol Chem 1992;267:31–4.
[70] Mundell SJ, Benovic JL. Selective regulation of endogenous G protein-coupled receptors by arrestins in HEK293 cells. J Biol Chem 2000;275:12900–8.
[71] Collison DJ, Coleman RA, James RS, Carey J, Duncan G. Characterization of muscarinic receptors in human lens cells by pharmacologic and molecular techniques. Invest Ophthalmol Vis Sci 2000;41:2633–41.
[72] Shaw G, Morse S, Ararat M, Graham FL. Preferential transformation of human neuronal cells by human adenoviruses and the origin of HEK 293 cells. FASEB J 2002;16:869–71.
[73] Williams ME, Burton B, Urrutia A, Shcherbatko A, Chavez-Noriega LE, Cohen CJ, et al. Ric-3 promotes functional expression of the nicotinic acetylcholine receptor alpha7 subunit in mammalian cells. J Biol Chem 2005;280:1257–63.
[74] Wang F, Gerzanich V, Wells GB, Anand R, Peng X, Keyser K, et al. Assembly of human neuronal nicotinic receptor alpha5 subunits with alpha3, beta2, and beta4 subunits. J Biol Chem 1996;271:17656–65.
[75] Dajas-Bailador FA, Mogg AJ, Wonnacott S. Intracellular Ca^{2+} signals evoked by stimulation of nicotinic acetylcholine receptors in SH-SY5Y cells: contribution of voltage-operated Ca^{2+} channels and Ca^{2+} stores. J Neurochem 2002;81:606–14.
[76] Cachelin AB, Rust G. Unusual pharmacology of (+)-tubocurarine with rat neuronal nicotinic acetylcholine receptors containing beta 4 subunits. Mol Pharmacol 1994;46:1168–74.
[77] Luo S, Kulak JM, Cartier GE, Jacobsen RB, Yoshikami D, Olivera BM, et al. alpha-conotoxin AuIB selectively blocks alpha3 beta4 nicotinic acetylcholine receptors and nicotine-evoked norepinephrine release. J Neurosci 1998;18:8571–9.
[78] Hofstra CL, Desai PJ, Thurmond RL, Fung-Leung WP. Histamine H4 receptor mediates chemotaxis and calcium mobilization of mast cells. J Pharmacol Exp Ther 2003;305:1212–21.
[79] Bongers G, Sallmen T, Passani M, Mariottini C, Wendelin D, Lozada Aea. New signaling pathways for the histamine H3 receptor. In: Proceedings of the XXXVth Annual Meeting of European Histamine Research Society; 2006.
[80] Koizumi H, Ohkawara A. H2 histamine receptor-mediated increase in intracellular Ca^{2+} in cultured human keratinocytes. J Dermatol Sci 1999;21: 127–32.
[81] Mitsuhashi M, Payan DG. Characterization of functional histamine H1 receptors on a cultured smooth muscle cell line. J Cell Physiol 1988; 134:367–75.
[82] Mitsuhashi M, Mitsuhashi T, Payan DG. Multiple signaling pathways of histamine H2 receptors. Identification of an H2 receptor-dependent Ca^{2+} mobilization pathway in human HL-60 promyelocytic leukemia cells. J Biol Chem 1989;264:18356–62.
[83] Lovenberg TW, Pyati J, Chang H, Wilson SJ, Erlander MG. Cloning of rat histamine H(3) receptor reveals distinct species pharmacological profiles. J Pharmacol Exp Ther 2000;293:771–8.
[84] Liu C, Wilson SJ, Kuei C, Lovenberg TW. Comparison of human, mouse, rat, and guinea pig histamine H4 receptors reveals substantial pharmacological species variation. J Pharmacol Exp Ther 2001;299:121–30.
[85] Soria-Jasso LE, Bahena-Trujillo R, Arias-Montano JA. Histamine H1 receptors and inositol phosphate formation in rat thalamus. Neurosci Lett 1997;225:117–20.
[86] Krzan M, Erjavec F, Carman-Krzan M. Characterization of coexistent histamine H1- and H2-receptor binding sites in the purified guinea pig myocardial membranes from ventricles. Inflamm Res 1993;38:C289–91.
[87] Vincent JP, Mazella J, Kitabgi P. Neurotensin and neurotensin receptors. Trends Pharmacol Sci 1999;20:302–9.
[88] Thomas P, Smart TG. HEK293 cell line: a vehicle for the expression of recombinant proteins. J Pharmacol Toxicol Methods 2005;51:187–200.
[89] Park TJ, Kim KT. Activation of B2 bradykinin receptors by neurotensin. Cell Signal 2003;15:519–27.
[90] Richard F, Barroso S, Martinez J, Labbe-Jullie C, Kitabgi P. Agonism, inverse agonism, and neutral antagonism at the constitutively active human neurotensin receptor 2. Mol Pharmacol 2001;60:1392–8.
[91] Larsson KP, Hansen AJ, Dissing S. The human SH-SY5Y neuroblastoma cell-line expresses a functional P2X7 purinoceptor that modulates voltage-dependent Ca^{2+} channel function. J Neurochem 2002;83:285–98.
[92] Daaka Y, Luttrell LM, Lefkowitz RJ. Switching of the coupling of the beta2-adrenergic receptor to different G proteins by protein kinase A. Nature 1997;390:88–91.
[93] Yarwood SJ, Woodgett JR. Extracellular matrix composition determines the transcriptional response to epidermal growth factor receptor activation. Proc Natl Acad Sci USA 2001;98:4472–7.
[94] Jong YJ, Schwetye KE, O'Malley KL. Nuclear localization of functional metabotropic glutamate receptor mGlu1 in HEK293 cells and cortical neurons: role in nuclear calcium mobilization and development. J Neurochem 2007;101:458–69.
[95] Kusano K, Gainer H. Modulation of voltage-activated Ca currents by pain-inducing agents in a dorsal root ganglion neuronal line, F-11. J Neurosci Res 1993;34:158–69.